

LINEAR LAVRENT'EV INTEGRAL EQUATION FOR THE NUMERICAL SOLUTION OF A NONLINEAR COEFFICIENT INVERSE PROBLEM*

MICHAEL V. KLIBANOV[†], JINGZHI LI[‡], AND WENLONG ZHANG[§]

Abstract. For the first time, we develop a convergent numerical method for the linear integral equation derived by M.M. Lavrent'ev in 1964 with the goal to solve a coefficient inverse problem for a wave-like equation in 3D. The data are non overdetermined. Convergence analysis is presented along with the numerical results. An intriguing feature of the Lavrent'ev equation is that, without any linearization, it reduces a highly nonlinear coefficient inverse problem to a linear integral equation of the first kind. Nevertheless, numerical results for that equation, which use the data generated for that coefficient inverse problem, show a good reconstruction accuracy. This is similar with the classical Gelfand-Levitan equation derived in 1951, which is valid in the 1D case.

Key words. coefficient inverse problem, Lavrent'ev equation, non overdetermined data, Carleman estimate, quasi-reversibility method, convergence rate

AMS subject classifications. 35R30

1. Introduction. A member of The Russian Academy of Science Mikhail M. Lavrent'ev (1932-2010) was one of founders of the theory of Ill-Posed and Inverse Problems. He was a Thesis Advisor of M.V. Klibanov. In 1964, when trying to solve a 3D Coefficient Inverse Problem (CIP) for the hyperbolic equation (2.5), Lavrent'ev has discovered a linear integral equation of the first kind, which solves that CIP [28], also see this equation in formula (7.18) of the book of Lavrent'ev, Romanov and Shishatskii [29]. The truly intriguing point of the Lavrent'ev's idea is that even though that equation is linear and also no linearization is made to derive it, still that equation solves a highly nonlinear CIP for PDE (2.5). However, the questions about the numerical method and image quality resulting from the numerical solution of that equation remained open. Thus, the goal of this paper is to address the following question: *Is it possible to obtain good quality images via a numerical solution of the linear Lavrent'ev equation using the measured data for that nonlinear CIP?* Surprisingly, the answer is positive.

In fact, this positive answer is similar with the answer for the classical Gelfand-Levitan (GL) linear integral equation of the second kind [30], which was first derived in 1951 for a CIP for a 1D differential equation [7]. Indeed, it was established numerically by Kabanikhin, Satybev and Shishlenin in [9] that numerical reconstruction results via the GL equation for the data generated by the solution of the forward problem

*Submitted to the editors DATE.

Funding: The effort of Klibanov was supported by US Army Research Laboratory and US Army Research Office grant W911NF-19-1-0044. The work of Li was partially supported by the NSF of China No. 11971221 and the Shenzhen Sci-Tech Fund No. JCYJ20170818153840322 and JCYJ20190809150413261. The work of Zhang was partially supported by the Shenzhen Sci-Tech Fund No. JCYJ20170818153840322, JCYJ20180307151603959 and the NSF of China No. 11901282 and 11731006.

[†]Department of Mathematics and Statistics, University of North Carolina at Charlotte, Charlotte, NC 28223, USA (mklibanv@uncc.edu)

[‡]Department of Mathematics, Southern University of Science and Technology (SUSTech), 1088 Xueyuan Boulevard, University Town of Shenzhen, Xili, Nanshan, Shenzhen, Guangdong Province, P.R.China (li.jz@sustech.edu.cn)

[§]Department of Mathematics, Southern University of Science and Technology (SUSTech), 1088 Xueyuan Boulevard, University Town of Shenzhen, Xili, Nanshan, Shenzhen, Guangdong Province, P.R.China (zhangwl@sustech.edu.cn)

for that differential equation are quite accurate ones.

The above mentioned CIP is concerned with the determination of the dielectric constant of the medium from some boundary measurements. In the case of the backscattering data, this CIP has direct applications in the problem of detection and identification of land mines and improvised explosive devices, see, e.g. [13, 14, 21] for reconstructions from experimentally collected data. There is also an interesting problem of the inspection of buildings using non invasive measurements of the electromagnetic field [26, 31]. In this case, measurements of both backscattering and transmitted signals can be carried out, and a corresponding CIP for equation (2.5) is supposed to be solved.

Ramm has used the Lavrent'ev equation to prove a uniqueness theorem for a CIP with overdetermined data [32]. As to the numerical studies, we refer to the work of Bakushinskii and Leonov [1]. In [1] non overdetermined data for the Lavrent'ev equation are considered. Since that equation is a linear integral equation of the first kind, then the problem of its solution is an ill-posed one. Hence, the numerical method of [1] searches for the so-called normal solution, see, e.g. [35] for normal solutions. The computed images of [1] are quite impressive ones. Nevertheless, convergence of the regularized solutions to the exact one was not proven in [1]. We also refer to [2] for a similar idea.

In this paper we consider the Lavrent'ev equation for the case of the non overdetermined data. We construct a radically new numerical method for this equation. For the first time, we derive from that equation a boundary value problem (BVP) for a system of coupled elliptic PDEs with overdetermined boundary conditions. In this derivation, we explore the orthonormal basis in the L_2 space, which was originally introduced in [18]. To solve that BVP, we use the Quasi-Reversibility Method (QRM), which was first introduced by Lattes and Lions [27]. Also, see [16] for the recent survey on this method. In addition, we refer to [4, 5] and references to these authors cited therein for some fresh ideas related to the QRM.

To analyze our specific version of the QRM, we establish first existence and uniqueness of the regularized solution of the QRM. Next, we turn to a much more difficult issue of establishing the convergence rate of the regularized solutions to the exact solution when the level of the noise in the data tends to zero. To do this, we use the Carleman estimate of [20]. We recall that Carleman estimates were used in [16] to establish convergence rates of regularized solutions of the QRM. However, the technique of this paper is quite different from the one of [16]. First, we do not use a cut-off function, unlike (2.15) in [16]. Second, our convergence rate is in the H^2 norm rather than in the weaker H^1 norm of [16]. The use of the H^2 norm is important here since it enables us to estimate the convergence rate of resulting solutions of the Lavrent'ev equation. Finally, our Carleman Weight Function is significantly different from the one in section 3 of [16]. This allows us to obtain convergence estimate in such a subdomain of the original domain of interest Ω , which is larger than a paraboloidal subdomain of [16], also see Remark 7.1 of section 7 for a relevant statement.

Since its first inception in [18], the above mentioned orthonormal basis in L_2 was successfully used by this research group for numerical solutions of linear inverse source problems for PDEs [22, 25, 34] as well as for some versions of the globally convergent convexification method for CIPs [12, 13, 14, 19, 23, 24].

We end up with presenting numerical results which solve CIPs for that hyperbolic PDE using the Lavrent'ev equation.

In section 2 we derive the Lavrent'ev equation from a CIP for a hyperbolic PDE. In section 3 we briefly review the above mentioned orthonormal basis. In section 4,

we derive that BVP for a system of linear coupled elliptic PDEs. In section 5, we introduce the QRM for that BVP. In section 6, we formulate Carleman estimates. In section 7 we provide convergence analysis for the BVP. Numerical studies are carried out in section 8.

2. Derivation of the Lavrent'ev Equation. Our derivation is different in some respects from the one of Lavrent'ev in [28]. Below $\mathbf{x} = (x, y, z) \in \mathbb{R}^3$. Let the numbers $A, b, d > 0$. Let the domain $\Omega \subset \mathbb{R}^3$ be a cube,

$$(2.1) \quad \Omega = \{\mathbf{x} = (x, y, z) : -A < x, y, z < A\}.$$

Let L_s be a line of locations of point sources \mathbf{x}_0 , and this line is located below the cube Ω ,

$$(2.2) \quad L_s = \{\mathbf{x}_0 = (x_0, 0, -A - b), \quad -d < x_0 < d\}.$$

Let the function $c(\mathbf{x})$ be sufficiently smooth in \mathbb{R}^3 and also

$$(2.3) \quad c(\mathbf{x}) \geq 1 \text{ in } \mathbb{R}^3,$$

$$(2.4) \quad c(\mathbf{x}) = 1 \text{ in } \mathbb{R}^3 \setminus \Omega.$$

Consider the following Cauchy problem

$$(2.5) \quad c(\mathbf{x}) u_{tt} = \Delta u, \quad \mathbf{x} \in \mathbb{R}^3, t > 0,$$

$$(2.6) \quad u(\mathbf{x}, 0) = 0, u_t(\mathbf{x}, 0) = \delta(\mathbf{x} - \mathbf{x}_0).$$

Coefficient Inverse Problem (CIP). Let $S \subset \mathbb{R}^3$ be a finite part of a plane and $S \cap \bar{\Omega} = S \cap L_s = \emptyset$. Find the function $c(\mathbf{x})$ for $\mathbf{x} \in \Omega$, given the functions $p_0(\mathbf{x}, \mathbf{x}_0, t)$ and $p_1(\mathbf{x}, \mathbf{x}_0, t)$,

$$(2.7) \quad u(\mathbf{x}, \mathbf{x}_0, t) = p_0(\mathbf{x}, \mathbf{x}_0, t), \quad (\mathbf{x}, \mathbf{x}_0, t) \in S \times L_s \times (0, \infty),$$

$$(2.8) \quad \frac{\partial}{\partial n(\mathbf{x})} u(\mathbf{x}, \mathbf{x}_0, t) = p_1(\mathbf{x}, \mathbf{x}_0, t), \quad (\mathbf{x}, \mathbf{x}_0, t) \in S \times L_s \times (0, \infty),$$

where $n = n(\mathbf{x})$ is a unit normal vector to S at the point $\mathbf{x} \in S$.

We assume that the function $c(\mathbf{x})$ satisfies the non-trapping condition. In other words, for any bounded domain $G \subset \mathbb{R}^3$, any geodesic line generated by $c(\mathbf{x})$ and starting in G leaves this domain in a finite time, see the book of Vainberg [37]. In this case the function $u(\mathbf{x}, \mathbf{x}_0, t)$ decays exponentially as $t \rightarrow \infty$ together with its derivatives with respect to \mathbf{x}, t up to the second order, and this decay is uniform with respect to $\mathbf{x} \in G$ for any bounded domain $G \subset \mathbb{R}^3$, see Lemma 6 of Chapter 10 of the book [37] and Remark 3 after this lemma.

Relaying on these results, apply to the function u the Fourier transform with respect to t ,

$$(2.9) \quad w(\mathbf{x}, \mathbf{x}_0, k) = \int_0^{\infty} u(\mathbf{x}, \mathbf{x}_0, t) e^{ikt} dt, \quad k \geq 0.$$

Due to that exponential decay, one can differentiate the function $w(\mathbf{x}, \mathbf{x}_0, k)$ at least twice with respect to \mathbf{x} and infinitely many times with respect to k . Furthermore, these derivatives can be calculated under the integral sign. A combination of Theorem 3.3 of [36] and Theorem 6 of Chapter 9 of [37] ensures that

$$(2.10) \quad \Delta_{\mathbf{x}} w + k^2 w + k^2 (c(\mathbf{x}) - 1) w = -\delta(\mathbf{x} - \mathbf{x}_0),$$

$$(2.11) \quad \frac{\partial w}{\partial r} - ikw = o\left(\frac{1}{r}\right), \quad r \rightarrow \infty, r = |\mathbf{x} - \mathbf{x}_0|.$$

Denote

$$(2.12) \quad w_0(\mathbf{x} - \mathbf{x}_0, k) = \frac{\exp(ik|\mathbf{x} - \mathbf{x}_0|)}{4\pi|\mathbf{x} - \mathbf{x}_0|}.$$

It is well known that the function $w(\mathbf{x}, \mathbf{x}_0, k)$ satisfies the Lippmann-Schwinger integral equation [6]

$$(2.13) \quad w(\mathbf{x}, \mathbf{x}_0, k) = w_0(\mathbf{x} - \mathbf{x}_0, k) + k^2 \int_{\Omega} w_0(\mathbf{x} - \boldsymbol{\xi}, k) (c(\boldsymbol{\xi}) - 1) w(\boldsymbol{\xi}, \mathbf{x}_0, k) d\boldsymbol{\xi}.$$

Differentiate (2.13) twice with respect to k and then set $k = 0$. Denote

$$(2.14) \quad q(\mathbf{x}) = c(\mathbf{x}) - 1.$$

$$(2.15) \quad w^0(\mathbf{x}, \mathbf{x}_0) = \partial_k^2 w(\mathbf{x}, \mathbf{x}_0, k) |_{k=0}.$$

By (2.13) and (2.14)

$$(2.16) \quad w^0(\mathbf{x}, \mathbf{x}_0) = - \int_0^{\infty} t^2 u(\mathbf{x}, \mathbf{x}_0, t) dt.$$

It follows from (2.12)-(2.15) that

$$(2.17) \quad \frac{1}{8\pi^2} \int_{\Omega} \frac{q(\boldsymbol{\xi})}{|\mathbf{x} - \boldsymbol{\xi}| |\boldsymbol{\xi} - \mathbf{x}_0|} d\boldsymbol{\xi} = w^0(\mathbf{x}, \mathbf{x}_0) - \frac{|\mathbf{x} - \mathbf{x}_0|}{4\pi}.$$

Equation (2.17) with respect to the function $q(\mathbf{x})$ is the Lavrent'ev equation.

We now reformulate the CIP (2.7), (2.8) in terms of equation (2.17). Denote

$$(2.18) \quad f_0(\mathbf{x}, \mathbf{x}_0) = - \int_0^{\infty} p_0(\mathbf{x}, \mathbf{x}_0, t) t^2 dt - \frac{|\mathbf{x} - \mathbf{x}_0|}{4\pi}, \quad \text{for } (\mathbf{x}, \mathbf{x}_0) \in S \times L_s,$$

$$(2.19) \quad f_1(\mathbf{x}, \mathbf{x}_0) = - \int_0^{\infty} p_1(\mathbf{x}, \mathbf{x}_0, t) t^2 dt - \frac{\partial}{\partial n(\mathbf{x})} \left(\frac{|\mathbf{x} - \mathbf{x}_0|}{4\pi} \right), \quad \text{for } (\mathbf{x}, \mathbf{x}_0) \in S \times L_s.$$

Denote

$$(2.20) \quad g_0(\mathbf{x}, \mathbf{x}_0) = 2\pi f_0(\mathbf{x}, \mathbf{x}_0) - \frac{|\mathbf{x} - \mathbf{x}_0|}{2}, \quad \text{for } (\mathbf{x}, \mathbf{x}_0) \in S \times L_s,$$

$$(2.21) \quad g_1(\mathbf{x}, \mathbf{x}_0) = 2\pi f_1(\mathbf{x}, \mathbf{x}_0) - \frac{\partial}{\partial n(\mathbf{x})} \left(\frac{|\mathbf{x} - \mathbf{x}_0|}{2} \right), \text{ for } (\mathbf{x}, \mathbf{x}_0) \in S \times L_s.$$

Then (2.17) implies:

$$(2.22) \quad \frac{1}{4\pi} \int_{\Omega} \frac{q(\boldsymbol{\xi})}{|\mathbf{x} - \boldsymbol{\xi}| |\boldsymbol{\xi} - \mathbf{x}_0|} d\boldsymbol{\xi} = g_0(\mathbf{x}, \mathbf{x}_0), \text{ for } (\mathbf{x}, \mathbf{x}_0) \in S \times L_s,$$

$$(2.23) \quad \frac{\partial}{\partial n(\mathbf{x})} \left(\frac{1}{4\pi} \int_{\Omega} \frac{q(\boldsymbol{\xi})}{|\mathbf{x} - \boldsymbol{\xi}| |\boldsymbol{\xi} - \mathbf{x}_0|} d\boldsymbol{\xi} \right) = g_1(\mathbf{x}, \mathbf{x}_0), \text{ for } (\mathbf{x}, \mathbf{x}_0) \in S \times L_s.$$

Therefore, we have reduced the CIP (2.7), (2.8) to the following inverse problem:

Problem For The Lavrent'ev Equation to Solve. Find the function $q(\mathbf{x})$, $\mathbf{x} \in \Omega$ from functions $g_0(\mathbf{x}, \mathbf{x}_0)$ and $g_1(\mathbf{x}, \mathbf{x}_0)$ given in (2.22), (2.23).

Remarks 2.1:

1. Note that this problem is non overdetermined. Indeed, in this problem $m = n = 3$, where m is the number of free variables in the data and n is the number of free variables in the unknown function $q(\mathbf{x})$. On the other hand, $m > n$ in the overdetermined case.

2. It follows from (2.22) that the right hand side of this equation is a harmonic function outside of the domain Ω . If, for example $S = \partial\Omega$, then this function can be uniquely determined outside Ω by its boundary values $g_0(\mathbf{x}, \mathbf{x}_0)$ at S . Hence, in this case we do not need to assign the normal derivative $g_1(\mathbf{x}, \mathbf{x}_0)$ at S since it will be calculated using $g_0(\mathbf{x}, \mathbf{x}_0)$. However, since $S \neq \partial\Omega$ above, then we indeed need to assign $g_1(\mathbf{x}, \mathbf{x}_0)$ in (2.23).

3. Even though we have sometimes worked above with complex valued functions, since we will work from now on with equations (2.22), (2.23) with a real valued function q , then all functions below are real valued ones. Also, all function spaces below are spaces of real valued functions.

3. A Special Orthonormal Basis. Recall that by (2.2) the point source $\mathbf{x}_0 = (x_0, 0, -A - b) \in L_s$ and $x_0 \in (-d, d)$. Prior to the description of our numerical method, we present in this section a special orthonormal basis $\{\Psi_n(x_0)\}_{n=0}^{\infty}$ in $L_2(-d, d)$. This basis has the following two properties:

1. $\Psi_n \in C^1[-d, d]$, $\forall n = 1, 2, \dots$
2. Let $\{, \}$ be the scalar product in $L_2(-d, d)$. Denote $a_{mn} = \{\Psi'_n, \Psi_m\}$. Then the matrix $M_N = (a_{mn})_{m,n=0}^N$ is invertible for any $N = 1, 2, \dots$

Note that if one would use either the basis of standard orthonormal polynomials or the trigonometric basis, then the first derivative of the first element of either of them would be identically zero. Hence, the matrix M_N would not be invertible in this case.

For the convenience of the reader, we now describe that basis. Consider the set of functions $\{\xi_n(x_0)\}_{n=0}^{\infty} = \{x_0^n e^{x_0}\}_{n=0}^{\infty}$. This is a set of linearly independent functions. Besides, this set is complete in the space $L_2(-d, d)$. After applying the Gram-Schmidt orthonormalization procedure to this set, we obtain the orthonormal basis $\{\Psi_n(x_0)\}_{n=1}^{\infty}$ in $L_2(-d, d)$. In fact, the function $\Psi_n(x_0)$ has the form $\Psi_n(x_0) = P_n(x_0)e^{x_0}$, $\forall n \geq 1$, where P_n is a polynomial of the degree n . Thus, functions $\Psi_n(x_0)$ are polynomials which are orthonormal in $L_2(-d, d)$ with the weight e^{2x_0} . The matrix

M_N is invertible since $\det M_N = 1$. Indeed elements $a_{mn} = (\Psi'_n, \Psi_m)$ of this matrix are such that [18]

$$a_{mn} = \begin{cases} 1 & \text{if } m = n, \\ 0 & \text{if } m > n. \end{cases}$$

In principle, the Gram-Schmidt orthonormalization procedure is unstable. However, in all our above referenced past works where the above basis was used we have always managed to find such a number N that it was stable for this N . This means that N is the regularization parameter of this procedure.

Remark 3.1. *As soon as N is fixed, we work within the framework of an approximate mathematical model. Estimating convergence of our method at $N \rightarrow \infty$ is a very challenging problem which we cannot address at the moment. The underlying reason of this is the ill-posed nature of problem (2.22), (2.23). Still, our numerical reconstructions of section 8 are of a good quality. We point out that the similar approximate mathematical models are quite often used in the field of inverse and ill-posed problems without proofs of convergence at $N \rightarrow \infty$, again because of the ill-posed nature of corresponding problems. In this regard we refer to, e.g. works [8, 9, 10, 11] of the authors, who are not members of this research team. Numerical results in all these publications are quite good ones. More detailed discussions of this issue can be found in [12, 20]. Even though similar truncations were made in these [12, 20], still good quality images were obtained.*

4. Numerical Method for Problem (2.22), (2.23). Below for each Banach space Z and for each integer m , we denote Z_m the space of m -dimensional vectors $D = (D_1, \dots, D_m)$, $D_j \in Z$ with the norm

$$\|D\|_{Z_m} = \left(\sum_{j=1}^m \|D_j\|_Z^2 \right)^{1/2}.$$

Keeping in mind locations of point sources in (2.2), we assume below for the surface S that it is either the backscattering part of the boundary of the cube Ω in (2.1), $S = S_{bsc}$ or its transmitted part $S = S_{tr}$, where

$$(4.24) \quad S_{bsc} = \{\mathbf{x} = (x, y, z) : -A < x, y < A, z = -A\},$$

$$(4.25) \quad S_{tr} = \{\mathbf{x} = (x, y, z) : -A < x, y < A, z = A\}.$$

Denote

$$v(\mathbf{x}, \mathbf{x}_0) = 2\pi \left[w^0(\mathbf{x}, \mathbf{x}_0) - \frac{|\mathbf{x} - \mathbf{x}_0|}{4\pi} \right].$$

By (2.17)

$$(4.26) \quad v(\mathbf{x}, \mathbf{x}_0) = \frac{1}{4\pi} \int_{\Omega} \frac{q(\boldsymbol{\xi})}{|\mathbf{x} - \boldsymbol{\xi}| |\boldsymbol{\xi} - \mathbf{x}_0|} d\boldsymbol{\xi}.$$

Hence,

$$(4.27) \quad \Delta_{\mathbf{x}} v(\mathbf{x}, \mathbf{x}_0) = -\frac{q(\mathbf{x})}{|\mathbf{x} - \mathbf{x}_0|}, \quad \mathbf{x} \in \Omega, \mathbf{x}_0 \in L_s.$$

Also, by (2.22) and (2.23)

$$(4.28) \quad v(\mathbf{x}, \mathbf{x}_0) = g_0(\mathbf{x}, \mathbf{x}_0), \quad \mathbf{x} \in S, \mathbf{x}_0 \in L_s,$$

$$(4.29) \quad \frac{\partial}{\partial n(\mathbf{x})} v(\mathbf{x}, \mathbf{x}_0) = g_1(\mathbf{x}, \mathbf{x}_0), \quad \mathbf{x} \in S, \mathbf{x}_0 \in L_s.$$

Multiply both sides of (4.27) by $|\mathbf{x} - \mathbf{x}_0|$ and, slightly abusing one of notations of section 2, denote

$$(4.30) \quad u(\mathbf{x}, \mathbf{x}_0) = v(\mathbf{x}, \mathbf{x}_0) |\mathbf{x} - \mathbf{x}_0|, \quad \mathbf{x} \in \Omega, \mathbf{x}_0 \in L_s.$$

By (4.27)

$$(4.31) \quad |\mathbf{x} - \mathbf{x}_0| \Delta_{\mathbf{x}} v(\mathbf{x}, \mathbf{x}_0) = -q(\mathbf{x}), \quad \mathbf{x} \in \Omega, \mathbf{x}_0 \in L_s.$$

By (4.30) the left hand side of (4.31) can be rewritten as

$$(4.32) \quad \begin{aligned} |\mathbf{x} - \mathbf{x}_0| \Delta_{\mathbf{x}} v &= \Delta_{\mathbf{x}} (|\mathbf{x} - \mathbf{x}_0| v) - 2 \nabla (|\mathbf{x} - \mathbf{x}_0|) \nabla v - \Delta (|\mathbf{x} - \mathbf{x}_0|) v \\ &= \Delta_{\mathbf{x}} u - 2 \frac{\mathbf{x} - \mathbf{x}_0}{|\mathbf{x} - \mathbf{x}_0|^2} \nabla_{\mathbf{x}} u + \frac{4}{|\mathbf{x} - \mathbf{x}_0|^2} u. \end{aligned}$$

To improve the stability of our method, we set:

$$(4.33) \quad \frac{\partial}{\partial n(\mathbf{x})} u(\mathbf{x}, \mathbf{x}_0) = \begin{cases} 0 & \text{for } \mathbf{x} \in S_{tr} \text{ if } S = S_{bsc}, \\ 0 & \text{for } \mathbf{x} \in S_{bsc} \text{ if } S = S_{tr}, \\ 0 & \text{for } \mathbf{x} \in \{x, y = \pm A, z \in (-A, A)\}, \end{cases} \quad \mathbf{x}_0 \in L_s.$$

It follows from (4.24), (4.25) and (4.26) that conditions (4.33) are approximately satisfied if the number A is sufficiently large and the support of $q(\mathbf{x})$ is far from the boundary $\partial\Omega$.

Next, (2.2), (4.30) and (4.32) imply that (4.27) is equivalent with

$$(4.34) \quad \Delta_{\mathbf{x}} u - \frac{2}{(x - x_0)^2 + y^2 + z^2} ((x - x_0) u_x + y u_y + z u_z - 2u) = -\frac{q(x, y, z)}{2\pi},$$

where $(x, y, z) \in \Omega, x_0 \in (-d, d)$. Differentiate both sides of (4.34) with respect to x_0 . We obtain for $(x, y, z) \in \Omega, x_0 \in (-d, d)$:

$$(4.35) \quad \Delta_{\mathbf{x}} u_{x_0} - 2 \frac{\partial}{\partial x_0} \left[\frac{(x - x_0) u_x + y u_y + z u_z - 2u}{(x - x_0)^2 + y^2 + z^2} \right] = 0.$$

We now represent the function $u(\mathbf{x}, \mathbf{x}_0) = u(x, y, z, x_0)$ as a truncated Fourier series with respect to the basis $\{\Psi_n(x_0)\}$,

$$(4.36) \quad u(x, y, z, x_0) = \sum_{n=1}^N u_n(x, y, z) \Psi_n(x_0),$$

$$(4.37) \quad u_{x_0}(x, y, z, x_0) = \sum_{n=1}^N u_n(x, y, z) \Psi'_n(x_0),$$

for $(x, y, z) \in \Omega, x_0 \in (-d, d)$. Here the number $N > 1$ should be chosen numerically. Therefore, coefficients $u_n(x, y, z)$ of the Fourier expansion (4.36) are unknown now, and we should focus on the search for these functions.

Substituting (4.36) and (4.37) in (4.35), we obtain for $\mathbf{x} \in \Omega, x_0 \in (-d, d)$

$$(4.38) \quad \sum_{n=1}^N \Delta_{\mathbf{x}} u_n(\mathbf{x}) \Psi'_n(x_0) - \frac{\partial}{\partial x_0} \left\{ \frac{2}{|\mathbf{x} - \mathbf{x}_0|^2} \sum_{n=1}^N [(\mathbf{x} - \mathbf{x}_0) \nabla u_n(\mathbf{x}) - 2u_n(\mathbf{x})] \Psi_n(x_0) \right\} = 0.$$

Multiply both sides of (4.38) sequentially by functions $\Psi_m(x_0), m = 1, \dots, N$ and integrate then with respect to $x_0 \in (-d, d)$. Denote the n -D vector of unknown coefficients in (4.36) as $U(\mathbf{x}) = (u_1, \dots, u_N)^T(\mathbf{x})$. We obtain a system of coupled elliptic equations of the second order,

$$(4.39) \quad L(U) = \Delta U + A_1(\mathbf{x})U_x + A_2(\mathbf{x})U_y + A_3(\mathbf{x})U_z + A_0(\mathbf{x})U = 0,$$

where $A_j(\mathbf{x}) \in C_{N^2}(\bar{\Omega})$ are $N \times N$ matrices. It follows from (4.28) and (4.29) that the following boundary vector functions $\varphi_0(\mathbf{x}), \varphi_1(\mathbf{x})$ are known:

$$(4.40) \quad U(\mathbf{x}) = \varphi_0(\mathbf{x}), \quad \frac{\partial}{\partial n(\mathbf{x})} U(\mathbf{x}) = \varphi_1(\mathbf{x}) \text{ for } \mathbf{x} \in S.$$

In addition (4.33) implies that

$$(4.41) \quad \frac{\partial}{\partial n(\mathbf{x})} U(\mathbf{x}) = 0 \text{ for } \mathbf{x} \in \{|x|, |y| = A, z \in (-A, A)\},$$

$$(4.42) \quad \frac{\partial}{\partial n(\mathbf{x})} U(\mathbf{x}) = 0 \text{ for } \mathbf{x} \in S_{tr} \text{ if } S = S_{bsc},$$

$$(4.43) \quad \frac{\partial}{\partial n(\mathbf{x})} U(\mathbf{x}) = 0 \text{ for } \mathbf{x} \in S_{bsc} \text{ if } S = S_{tr}.$$

Thus, depending on the location of the surface S : whether $S = S_{bsc}$ or $S = S_{tr}$, we actually got two boundary value problems:

Boundary Value Problem 1 (BVP1). Solve system (4.39) with the boundary conditions (4.40)-(4.42).

Boundary Value Problem 2 (BVP2). Solve system (4.39) with the boundary conditions (4.40), (4.41), (4.43).

Remark 4.1. Since we have the Cauchy data at the surface S in (4.40) for the elliptic system (4.39), then each of these BVPs has at most one solution. This follows from the classical unique continuation theorem for elliptic PDEs, see, e.g. Chapter 4 of [29].

5. The Quasi-Reversibility Method For Problems 1,2. Both these problems are overdetermined ones due to the overdetermination of the boundary data (4.40). Thus, we solve both problems via the Quasi-Reversibility Method (QRM),

which is well suitable for solving overdetermined BVPs for PDEs. Following the survey [16] on the QRM, we consider two minimization problems. We remind that a significant difference with [16] is in the convergence Theorem 7.2.

Denote $\partial_1\Omega = \partial\Omega \setminus \{z = A\}$, $\partial_2\Omega = \partial\Omega \setminus \{z = -A\}$. Introduce two subspaces of the space $H^3(\Omega)$,

$$(5.44) \quad \begin{aligned} H_{0,bsc}^3(\Omega) &= \{u \in H^3(\Omega) : u|_{S_{bsc}} = \partial_{n(\mathbf{x})}u|_{\partial_1\Omega} = 0\}, \\ H_{0,tr}^3(\Omega) &= \{u \in H^3(\Omega) : u|_{S_{tr}} = \partial_{n(\mathbf{x})}u|_{\partial_2\Omega} = 0\}. \end{aligned}$$

To solve BVPs 1 and 2, we consider Minimization Problems 1 and 2 respectively. Below $\mathbf{x} = (x, y, z)$. We assume that, in the case of BVP 1, there exists such a vector function $F_1 \in H_N^3(\Omega)$ that satisfies boundary conditions (4.40)-(4.42). And in the case of Problem 2, we assume the existence of such a function $F_2 \in H_N^3(\Omega)$ that satisfies boundary conditions (4.40), (4.41), (4.43). Denote

$$(5.45) \quad \begin{cases} V = U - F_1 \text{ in the case of BVP1,} \\ W = U - F_2 \text{ in the case of BVP2.} \end{cases}$$

Hence, $V \in H_{0,bsc,N}^3(\Omega)$ and $W \in H_{0,tr,N}^3(\Omega)$.

Minimization Problem 1. Let L be the operator in (4.39). Minimize the functional J_γ on the space $H_{0,bsc,N}^3(\Omega)$,

$$(5.46) \quad J_\gamma(V) = \int_{\Omega} |L(V + F_1)|^2 d\mathbf{x} + \gamma \|V\|_{H_N^3(\Omega)}^2.$$

Here $\gamma \in (0, 1)$ is the regularization parameter.

Minimization Problem 2. Minimize the functional I_γ on the space $H_{0,tr,N}^3(\Omega)$

$$(5.47) \quad I_\gamma(W) = \int_{\Omega} |L(W + F_2)|^2 d\mathbf{x} + \gamma \|W\|_{H_N^3(\Omega)}^2.$$

Remark 5.1. As soon as a minimizer of either of these functionals is found, we reconstruct the vector function U by either of formulas (5.45). Then we reconstruct the function $u(x, y, z, x_0)$ via (4.36) and then reconstruct the target function $q(x, y, z)$ via (4.34). In our computations we use $x_0 = 0$ to reconstruct q via (4.34).

6. Carleman Estimates. Let $\lambda \geq 1$ be a parameter, which is always used in CWFs and let the number $R > A$. Introduce two CWFs $\mu_{1,\lambda}(z)$ and $\mu_{2,\lambda}(z)$ for the Minimization Problems 1 and 2 respectively,

$$(6.48) \quad \mu_{1,\lambda}(z) = \exp\left(\lambda(z - R)^2\right), z \in (-A, A),$$

$$(6.49) \quad \mu_{2,\lambda}(z) = \exp\left(\lambda(z + R)^2\right), z \in (-A, A).$$

Hence, $\mu'_{1,\lambda}(z) < 0$ for $z \in [-A, A]$ and $\mu'_{2,\lambda}(z) > 0$ for $z \in [-A, A]$. This means that the function $\mu_{1,\lambda}(z)$ is decreasing for $z \in [-A, A]$ and the function $\mu_{2,\lambda}(z)$ is increasing for $z \in [-A, A]$. Below $C = C(A, R) > 0$ denotes different constants depending only on the number A in (2.1). Also, $B = B(A, R, L) > 0$ denotes different

constants depending only on numbers A, R and the maximum of $C_{N^2}(\bar{\Omega})$ –norms of matrices of the operator L in (4.39).

Theorem 6.1 (Carleman estimate) *There exists constants $\lambda_0 = \lambda_0(A) > 1$ and $C = C(A, R) > 0$ such that the following Carleman estimate holds for all functions $u \in H_{0,bsc}^3(\Omega)$ and for all $\lambda \geq \lambda_0$:*

$$(6.50) \quad \int_{\Omega} (\Delta u)^2 \mu_{1,\lambda}^2 d\mathbf{x} \geq \frac{C}{\lambda} \sum_{i,j=1}^3 \int_{\Omega} u_{x_i x_j}^2 \mu_{1,\lambda}^2 d\mathbf{x} + C\lambda \int_{\Omega} (|\nabla u|^2 + \lambda^2 u^2) \mu_{1,\lambda}^2 d\mathbf{x} \\ - C\lambda^3 e^{2\lambda(A-R)^2} \|u\|_{H^3(\Omega)}^2.$$

Theorem 6.2 (Carleman estimate). *There exists constants $\lambda_0 = \lambda_0(A) > 0$ and $C = C(A, R) > 0$ such that the following Carleman estimate holds for all functions $u \in H_{0,tr}^3(\Omega)$ and for all $\lambda \geq \lambda_0$:*

$$\int_{\Omega} (\Delta u)^2 \mu_{2,\lambda}^2 d\mathbf{x} \geq \frac{C}{\lambda} \sum_{i,j=1}^3 \int_{\Omega} u_{x_i x_j}^2 \mu_{2,\lambda}^2 d\mathbf{x} + C\lambda \int_{\Omega} (|\nabla u|^2 + \lambda^2 u^2) \mu_{2,\lambda}^2 d\mathbf{x} \\ - C\lambda^3 e^{2\lambda(A+R)^2} \|u\|_{H^3(\Omega)}^2.$$

The proof of each of these theorems is a slight modification of the proof of Theorem 4.1 of our work [20], and then this modification should be combined with the trace theorem. Hence, we do not prove Theorems 6.1 and 6.2 here.

7. Convergence Analysis of the QRM. For brevity, we provide in this section convergence analysis only for the Minimization Problem 1, since this analysis is completely similar for the Minimization Problem 2. The only difference is that we need to use Theorem 6.2 instead of Theorem 6.1 in the second case.

7.1. Existence and uniqueness of the minimizer. Theorem 7.1. *Consider the Minimization Problem 1. For any $\gamma > 0$ there exists unique minimizer $V_{\min} \in H_{0,bsc,N}^3(\Omega)$ of the functional $J_{\gamma}(V)$ and the following estimate holds*

$$\|V_{\min}\|_{H_N^3(\Omega)} \leq \frac{C}{\sqrt{\gamma}} \|F_1\|_{H_N^3(\Omega)}.$$

The minimizer of Theorem 7.1 is called “regularized solution” in the regularization theory [3, 35]. This theorem follows immediately from Theorem 2.4 of [16]. That theorem was proved using the variational principle and the Riesz theorem. However, to establish convergence rate of the regularized solutions to the exact one when the level of noise in the data tends to zero, we need to apply in the next subsection the Carleman estimate of Theorem 6.1.

7.2. Convergence rate of regularized solutions. Denote (\cdot, \cdot) and $[\cdot, \cdot]$ scalar products in spaces $L_2(\Omega)$ and $H^3(\Omega)$ respectively. As it is often the case in the theory of ill-posed problems, we assume that there exists exact solution $U^* \in H_N^3(\Omega)$ of equation (4.39) with noiseless boundary data $\varphi_0^*(\mathbf{x}), \varphi_1^*(\mathbf{x})$ in (4.40) and satisfying additional boundary conditions (4.41)-(4.43). Since such a vector function U^* exists, then there also exists a vector function $F_1^* \in H_N^3(\Omega)$ satisfying these noiseless boundary conditions (4.40) as well as additional zero Neumann boundary conditions (4.41)-(4.43).

Denote

$$(7.51) \quad V^* = U^* - F_1^*.$$

Then $V^* \in H_{0,bsc,N}^3(\Omega)$ and

$$(7.52) \quad L(V^* + F_1^*) = 0.$$

Let $\delta \in (0, 1)$ be the level of noise in the data. We assume that

$$(7.53) \quad \|F_1 - F_1^*\|_{H_N^2(\Omega)} \leq \delta.$$

Hence,

$$(7.54) \quad \|L(F_1) - L(F_1^*)\|_{L_{2,N}(\Omega)} \leq B\delta.$$

Let $\varepsilon \in (0, A)$ be an arbitrary number. Denote

$$\Omega_\varepsilon = \{\mathbf{x} = (x, y, z) : -A < x, y < A, z \in (-A, A - \varepsilon)\} \subset \Omega.$$

Theorem 7.2 (convergence rate of regularized solutions). *Let $\gamma = \gamma(\delta) = \delta^2$. Let $V_{\min,\delta} \in H_{0,bsc,N}^3(\Omega)$ be the minimizer of the functional $J_{\delta^2}(V)$, which is guaranteed by Theorem 7.1. Denote $U_{\min,\delta} = V_{\min,\delta} + F_1$. There exists a sufficiently small number $\delta_0 \in (0, 1)$ and a number $\alpha \in (0, 1/2)$ such that for all $\delta \in (0, \delta_0)$ the following convergence rate holds:*

$$(7.55) \quad \|U_{\min,\delta} - U^*\|_{H_N^2(\Omega_\varepsilon)} \leq B \left(1 + \|U^*\|_{H_N^3(\Omega)} + \|F_1^*\|_{H_N^3(\Omega)}\right) \delta^\alpha.$$

Remark 7.1. *The subdomain $\Omega_\varepsilon \subset \Omega$, where convergence estimate (7.55) is given, is larger than a paraboloidal subdomain of Ω , where the convergence estimate of Theorem 3.2 of [16] is given in the elliptic case.*

Proof of Theorem 7.2. It follows from the variational principle that

$$(7.56) \quad (L(V_{\min,\delta}), L(h)) + \delta^2 [V_{\min,\delta}, h] = -(L(F_1), L(h)), \quad \forall h \in H_{0,bsc,N}^3(\Omega).$$

Also, by (7.52)

$$(7.57) \quad (L(V^*), L(h)) + \delta^2 [V^*, h] = -(L(F_1^*), L(h)) + \delta^2 [V^*, h], \quad \forall h \in H_{0,bsc,N}^3(\Omega).$$

Denote $\tilde{V}_\delta = V_{\min,\delta} - V^*$ and $G_\delta = L(F_1^*) - L(F_1)$. By (7.54)

$$(7.58) \quad \|G_\delta\|_{L_{2,N}(\Omega)} \leq B\delta.$$

Subtract (7.57) from (7.56). We obtain

$$(7.59) \quad \begin{aligned} & \left(L(\tilde{V}_\delta), L(h) \right) + \delta^2 [\tilde{V}_\delta, h] \\ &= (G_\delta, L(h)) - \delta^2 [V^*, h], \quad \forall h \in H_{0,bsc,N}^3(\Omega). \end{aligned}$$

Setting in (7.59) $h = \tilde{V}_\delta$, we obtain

$$(7.60) \quad \left\| L(\tilde{V}_\delta) \right\|_{L_{2,N}(\Omega)}^2 + \delta^2 \left\| \tilde{V}_\delta \right\|_{H_N^3(\Omega)}^2 = \left(G_\delta, L(\tilde{V}_\delta) \right) - \delta^2 [V^*, \tilde{V}_\delta].$$

By the Cauchy-Schwarz inequality and (7.58),

$$\begin{aligned} \left(G_\delta, L(\tilde{V}_\delta) \right) - \delta^2 [V^*, \tilde{V}_\delta] &\leq B \frac{\delta^2}{2} + \frac{1}{2} \left\| L(\tilde{V}_\delta) \right\|_{L_{2,N}(\Omega)}^2 \\ &\quad + \frac{\delta^2}{2} \left\| \tilde{V}_\delta \right\|_{H_N^3(\Omega)}^2 + \frac{\delta^2}{2} \|V^*\|_{H_N^3(\Omega)}^2. \end{aligned}$$

Comparison of this with (7.60) gives

$$\left\| L(\tilde{V}_\delta) \right\|_{L_{2,N}(\Omega)}^2 + \delta^2 \left\| \tilde{V}_\delta \right\|_{H_N^3(\Omega)}^2 \leq B \left(1 + \|V^*\|_{H_N^3(\Omega)}^2 \right) \delta^2.$$

Hence,

$$(7.61) \quad \left\| \tilde{V}_\delta \right\|_{H_N^3(\Omega)}^2 \leq B \left(1 + \|V^*\|_{H_N^3(\Omega)}^2 \right),$$

$$(7.62) \quad \left\| L(\tilde{V}_\delta) \right\|_{L_{2,N}(\Omega)}^2 \leq B \left(1 + \|V^*\|_{H_N^3(\Omega)}^2 \right) \delta^2.$$

Keeping in mind (7.61), we will now work with (7.62),

$$\begin{aligned} \left\| L(\tilde{V}_\delta) \right\|_{L_{2,N}(\Omega)}^2 &= \int_{\Omega} \left[L(\tilde{V}_\delta) \right]^2 d\mathbf{x} = \int_{\Omega} \left[L(\tilde{V}_\delta) \right]^2 \mu_{1,\lambda}^2(z) e^{-2\lambda(z-R)^2} d\mathbf{x} \\ &\geq e^{-2\lambda(A+R)^2} \int_{\Omega} \left[L(\tilde{V}_\delta) \right]^2 \mu_{1,\lambda}^2(z) d\mathbf{x}. \end{aligned}$$

Hence, (7.62) implies

$$(7.63) \quad \int_{\Omega} \left[L(\tilde{V}_\delta) \right]^2 \mu_{1,\lambda}^2 d\mathbf{x} \leq B \left(1 + \|V^*\|_{H_N^3(\Omega)}^2 \right) e^{2\lambda(A+R)^2} \delta^2.$$

We now apply the Carleman estimate of Theorem 6.1 to the left hand side of (7.63) for all $\lambda \geq \lambda_0$,

$$\begin{aligned} \int_{\Omega} \left[L(\tilde{V}_\delta) \right]^2 \mu_{1,\lambda}^2 d\mathbf{x} &\geq \frac{1}{2} \int_{\Omega} (\Delta \tilde{V}_\delta)^2 \mu_{1,\lambda}^2 d\mathbf{x} - B \int_{\Omega} \left(|\nabla \tilde{V}_\delta|^2 + \tilde{V}_\delta^2 \right) \mu_{1,\lambda}^2 d\mathbf{x} \\ (7.64) \quad &\geq \frac{C}{\lambda} \sum_{i,j=1}^3 \int_{\Omega} \left(\partial_{x_i} \partial_{x_j} \tilde{V}_\delta \right)^2 \mu_{1,\lambda}^2 d\mathbf{x} + C\lambda \int_{\Omega} \left(|\nabla \tilde{V}_\delta|^2 + \lambda^2 \tilde{V}_\delta^2 \right) \mu_{1,\lambda}^2 d\mathbf{x} \\ &\quad - C\lambda^3 e^{2\lambda(A-R)^2} \left\| \tilde{V}_\delta \right\|_{H_N^3(\Omega)}^2 - B \int_{\Omega} \left(|\nabla \tilde{V}_\delta|^2 + \tilde{V}_\delta^2 \right) \mu_{1,\lambda}^2(z) d\mathbf{x}. \end{aligned}$$

Let the number $\lambda_1 \geq \lambda_0 > 1$ be such that $C\lambda_1 > 2B$. Then we obtain from (7.64) for all $\lambda \geq \lambda_1$ and with a different constant C

$$\int_{\Omega} \left[L(\tilde{V}_\delta) \right]^2 \mu_{1,\lambda}^2(z) d\mathbf{x} \geq \frac{C}{\lambda} \sum_{i,j=1}^3 \int_{\Omega} \left(\partial_{x_i} \partial_{x_j} \tilde{V}_\delta \right)^2 \mu_{1,\lambda}^2 d\mathbf{x} +$$

$$\begin{aligned}
& + C\lambda \int_{\Omega} \left(|\nabla \tilde{V}_{\delta}|^2 + \lambda^2 \tilde{V}_{\delta}^2 \right) \mu_{1,\lambda}^2 d\mathbf{x} - C\lambda^3 e^{2\lambda(A-R)^2} \left\| \tilde{V}_{\delta} \right\|_{H_N^3(\Omega)}^2 \\
& \geq e^{2\lambda(A-\varepsilon-R)^2} \frac{C}{\lambda} \sum_{i,j=1}^3 \int_{\Omega_{\varepsilon}} \left(\partial_{x_i} \partial_{x_j} \tilde{V}_{\delta} \right)^2 \mu_{1,\lambda}^2 d\mathbf{x} + e^{2\lambda(A-\varepsilon-R)^2} C \int_{\Omega_{\varepsilon}} \left(|\nabla \tilde{V}_{\delta}|^2 + \tilde{V}_{\delta}^2 \right) d\mathbf{x} - \\
& \quad - C\lambda^3 e^{2\lambda(A-R)^2} \left\| \tilde{V}_{\delta} \right\|_{H_N^3(\Omega)}^2.
\end{aligned}$$

Combining this estimate with (7.61) and (7.62), we obtain

$$\begin{aligned}
(7.65) \quad \left\| \tilde{V}_{\delta} \right\|_{H^2(\Omega_{\varepsilon})}^2 & \leq B \left(1 + \|V^*\|_{H_N^2(\Omega)}^2 \right) \lambda^4 \exp \left[2\lambda \left((A-R)^2 - (A-\varepsilon-R)^2 \right) \right] \\
& \quad + B \left(1 + \|V^*\|_{H_N^3(\Omega)}^2 \right) \lambda^4 e^{2\lambda(A+R)^2} \delta^2.
\end{aligned}$$

Choose $\lambda_2 \geq \lambda_1$ such that

$$(7.66) \quad \lambda^4 < e^{\lambda\varepsilon^2}, \quad \forall \lambda \geq \lambda_2.$$

Then

$$\begin{aligned}
(7.67) \quad \lambda^4 \exp \left[2\lambda \left((A-R)^2 - (A-\varepsilon-R)^2 \right) \right] \\
& < \exp \left\{ -2\lambda\varepsilon \left[2(R-A) + \frac{\varepsilon}{2} \right] \right\}.
\end{aligned}$$

By (7.65)-(7.67)

$$\begin{aligned}
(7.68) \quad \left\| \tilde{V}_{\delta} \right\|_{H^2(\Omega_{\varepsilon})}^2 & \leq B \left(1 + \|V^*\|_{H_N^3(\Omega)}^2 \right) \exp \left\{ -2\lambda\varepsilon \left[2(R-A) + \frac{\varepsilon}{2} \right] \right\} \\
& \quad + B \left(1 + \|V^*\|_{H_N^3(\Omega)}^2 \right) e^{2\lambda[(A+R)^2 + \varepsilon^2/2]} \delta^2.
\end{aligned}$$

Choose $\lambda = \lambda(\delta)$ such that

$$(7.69) \quad \exp \left[2\lambda \left((A+R)^2 + \varepsilon^2/2 \right) \right] \delta^2 = \delta.$$

Hence,

$$(7.70) \quad 2\lambda(\delta) = \ln \left(\delta^{[(A+R)^2 + \varepsilon^2/2]^{-1}} \right).$$

Hence, by the choice (7.70) we assume that δ_0 is so small that

$$\ln \left(\delta_0^{[(A+R)^2 + \varepsilon^2/2]^{-1}} \right) > 2\lambda_2.$$

We set $\delta \in (0, \delta_0)$. Hence,

$$\exp \left\{ -2\lambda(\delta)\varepsilon \left[2(R-A) + \frac{\varepsilon}{2} \right] \right\} = \delta^{2\alpha},$$

$$2\alpha = \frac{\varepsilon [2(R - A) + \varepsilon/2]}{(A + R)^2 + \varepsilon^2/2}.$$

Since $\varepsilon \in (0, A)$, then, using elementary calculations, we obtain

$$(7.71) \quad 2\alpha = \frac{\varepsilon [2(R - A) + \varepsilon/2]}{(A + R)^2 + \varepsilon^2/2} < 1.$$

Hence, (7.51), (7.68)-(7.70) and the triangle inequality imply

$$(7.72) \quad \begin{aligned} \left\| \tilde{V}_\delta \right\|_{H^2(\Omega_\varepsilon)} &\leq B \left(1 + \|V^*\|_{H_N^3(\Omega)} \right) \delta^\alpha \\ &\leq B \left(1 + \|U^*\|_{H_N^3(\Omega)} + \|F_1^*\|_{H_N^3(\Omega)} \right) \delta^\alpha. \end{aligned}$$

Now, since

$$\begin{aligned} \tilde{V}_\delta &= V_{\min, \delta} - V^* = (U_{\min, \delta} - F_1) - (U^* - F_1^*) = (U_{\min, \delta} - U^*) + (F_1^* - F_1) \\ &= (U_{\min, \delta} - U^*) + (F_1^* - F_1), \end{aligned}$$

then (7.53) and the triangle inequality imply that

$$(7.73) \quad \left\| \tilde{V}_\delta \right\|_{H^2(\Omega_\varepsilon)} \geq \|U_{\min, \delta} - U^*\|_{H^2(\Omega_\varepsilon)} - \delta.$$

Finally, since by (7.71) $\delta < \delta^\alpha$, then, using (7.72) and (7.73), we obtain (7.55) with a new constant B . \square

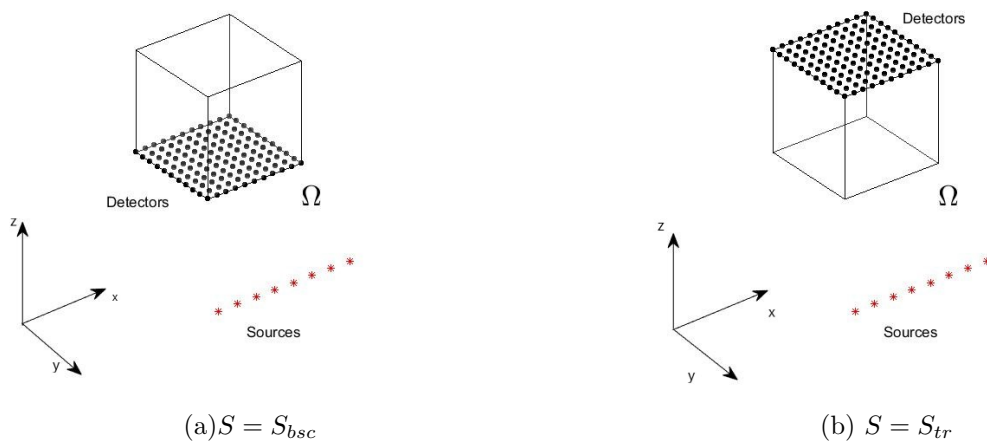
7.3. Convergence rate of functions $q(\mathbf{x})$. While Theorem 7.2 establishes convergence the rate of regularized solutions of the Minimization Problem 1, the next natural question is about the convergence rate of corresponding target functions $q(\mathbf{x})$, which are the approximate solutions of the system of integral equations (2.22), (2.23). Recall that these functions are reconstructed as described in Remark 5.1. Theorem 7.3 follows immediately from Remark 5.1 and Theorem 7.2.

Theorem 7.3. *Assume that all conditions of subsection 7.2, described above as well as of Theorem 7.2 hold. Let $q_{\min, \delta}(\mathbf{x})$ and $q^*(\mathbf{x})$ be the functions, which are reconstructed from the vector functions $U_{\min, \delta}$ and U^* respectively by the procedure described in Remark 5.1. Let the number $\alpha \in (0, 1/2)$ be the same as in Theorem 7.1. Then the following convergence rate holds:*

$$\|q_{\min, \delta} - q^*\|_{L_2(\Omega_\varepsilon)} \leq B \left(1 + \|U^*\|_{H_N^3(\Omega)} + \|F_1^*\|_{H_N^3(\Omega)} \right) \delta^\alpha.$$

8. Numerical Studies.

8.1. Numerical implementation. In all the numerical tests, we have chosen the numbers $A = 0.75$, $b = -5$ and $d = 1$ in (2.1) and (2.2). We have used 101 sources which are uniformly distributed on the line L_s and 10×10 detectors uniformly distributed on the surface S . See Figure 8.1 for a schematic diagram of domain Ω , sources and detectors when S is either the backscattering part $S = S_{b_{sc}}$ of the boundary of the cube Ω or its transmitted part $S = S_{tr}$.

FIG. 8.1. A schematic diagram of domain Ω , sources and detectors.

8.1.1. The forward problem (2.5), (2.6). To generate the data (2.18)-(2.21) for BVP1 and BVP2 of section 4, we have solved the forward problem (2.5), (2.6) for each of those 101 sources by the finite difference method. Since this procedure is very time consuming, due to a large number of sources, we have parallelized computations. The parallel computations were performed on 32 processors. The delta function $\delta(\mathbf{x} - \mathbf{x}_0)$ in (2.6) was modeled as

$$f(x - x^{(s)}) = \begin{cases} \frac{1}{\varepsilon} \exp\left(-\frac{1}{1 - \|x - x_s\|^2/\varepsilon}\right), & \text{if } \|x - x_s\|^2 < \varepsilon, \\ 0, & \text{otherwise.} \end{cases}$$

with $\varepsilon = 0.05$. In fact, we have found solution of equation (2.5) with initial conditions (2.6) in the cube

$$\Phi = \{\mathbf{x} = (x, y, z) : -10 < x, y, z < 10\}$$

with absorbing boundary conditions on the boundary of this cube.

The step sizes with respect to spatial and time variables were $h = 1/20$ and $\tau = 1/100$ respectively. We have used an implicit scheme. To approximate integrals (2.18), (2.19) over the infinite interval $t \in (0, \infty)$ we have continued computations of problem (2.5), (2.6) for each source position \mathbf{x}_0 until such a moment of time T for which $\|u(\mathbf{x}, \mathbf{x}_0, T)\|_{L^\infty} \leq 10^{-3}$, where the norm is understood in the discrete sense of grid of finite differences. We have found that $T = 10$ for all locations of the point source. Next, we replaced in integrals (2.18), (2.19) the integration interval $t \in (0, \infty)$ with the interval $t \in (0, T)$.

8.1.2. The inverse problem. Even though we use the $H_N^3(\Omega)$ -norm in the regularization terms in (5.46), (5.47), we have discovered numerically that the simpler $H_N^2(\Omega)$ -norm is sufficient. To minimize either of functionals (5.46), (5.47), we have written differential operators in them in the form of finite differences. Then we have minimized with respect to the values of the corresponding vector functions at grid points. The grid step size was $\tilde{h} = 1/10$. The discrete problems of (5.46), (5.47) will lead to 2 linear systems. Then we have solved the minimization problems (5.46), (5.47) directly by solving these 2 linear equations.

8.2. Results. In the tests of this subsection, we demonstrate the efficiency of our numerical method. We display on Figures 2-9 the function $q(\mathbf{x}) = c(\mathbf{x}) - 1$, see (2.14). In all tests the background value of $q_{bkg}(\mathbf{x}) = 0$, which corresponds to the background value of the dielectric constant $c_{bkg}(\mathbf{x}) = 1$. In all tests slices are depicted to demonstrate the values of the computed function $q(\mathbf{x})$. In our computations, we took the number of Fourier coefficients $N = 6$ in (4.36), (4.37).

In tests 1-4, we work with the case when the surface S is

$$S = S_{bsc} = \{\mathbf{x} : |x|, |y| < 0.75, z = -0.75\}$$

is the backscattering part of the boundary of the cube Ω , see Figure 1(a) and (4.24). In tests 1-3, we have noiseless data on S , and we set in these tests the regularization parameter $\gamma = 0$ in (5.46). In test 4 we use noisy data with the noise level $\delta = 0.05$ (i.e. 5%), and we set in test 4 $\gamma = 10^{-8}$ in (5.46).

Test 1. First, we test the reconstruction by our method of the case when the shape of our inclusion is the same as the shape of the number ‘1’. The function $q(\mathbf{x})$ is depicted on Figures 8.2 (a) and (b). $q = 1$ inside of this inclusion and $q = 0$ outside of it. See Figures 8.2 for the reconstruction results.

Test 2. We test the reconstruction by our method of three (3) single ball shaped inclusions with a high contrast, see Figures 8.3 (a) and (b). $q = 3$ inside of this inclusions and $q = 0$ outside of them. See Figures 8.3 for the results of the reconstruction.

Test 3. We test the reconstruction by our method of the case when the shape of our inclusion is the same as the shape of the letter ‘C’. The function $q(\mathbf{x})$ is depicted on Figures 8.4 (a) and (b). $q = 1$ inside of this inclusion and $q = 0$ outside of it. See Figures 8.4 for the reconstruction results.

Test 4. In this example, we test the stability of our algorithm with respect to the random noise in the data. We use the same function $q(\mathbf{x})$ as the one in Test 3. The random noise is added on S_{bsc} as:

$$g_{0,noise}(\mathbf{x}, \mathbf{x}_0) = g_0(\mathbf{x}, \mathbf{x}_0) + \delta \max_{\mathbf{x} \in S_{bsc}, \mathbf{x}_0 \in L_s} |g_0(\mathbf{x}, \mathbf{x}_0)| \xi_{\mathbf{x}_0}, \quad \mathbf{x} \in S_{bsc}, \mathbf{x}_0 \in L_s,$$

$$g_{1,noise}(\mathbf{x}, \mathbf{x}_0) = g_1(\mathbf{x}, \mathbf{x}_0) + \delta \max_{\mathbf{x} \in S_{bsc}, \mathbf{x}_0 \in L_s} |g_1(\mathbf{x}, \mathbf{x}_0)| \xi_{\mathbf{x}_0}, \quad \mathbf{x} \in S_{bsc}, \mathbf{x}_0 \in L_s,$$

where functions $g_0(\mathbf{x}, \mathbf{x}_0), g_1(\mathbf{x}, \mathbf{x}_0)$ are defined in (2.20), (2.21), δ is the noise level and $\xi_{\mathbf{x}_0}$ is a random variable depending only on the source position \mathbf{x}_0 and uniformly distributed on $[-1, 1]$. We took $\delta = 0.05$, which corresponds to 5% noise level. See Figures 8.5 for the reconstruction results.

In tests 5-8, we show the reconstruction results for the case when the surface S is

$$S = S_{tr} = \{\mathbf{x} : |x|, |y| < A, z = A\}$$

is the transmitted part of the boundary of the cube Ω , see Figure 1(b) and (4.25). In tests 5-7, the we use noiseless data S are set the regularization parameter $\gamma = 0$ in (5.47). In test 8 we consider the noisy data in the same manner as in test 5 with $\delta = 0.05$ and we set in (5.47) $\gamma = 10^{-8}$.

Test 5. First, we test the reconstruction by our method of the case when the shape of our inclusion is the same as the shape of the number ‘1’. The function $q(\mathbf{x})$ is depicted on Figures 8.6 (a) and (b). $q = 1$ inside of ‘1’ and $q = 0$ outside of it. See Figures 8.6 for the reconstruction results.

Test 6. We test the reconstruction by our method of three (3) ball shaped inclusions with high contrast, see Figures 8.7 (a), (b). $q = 3$ inside of these inclusions and $q = 0$ outside of them. See Figures 8.7 for the reconstruction results.

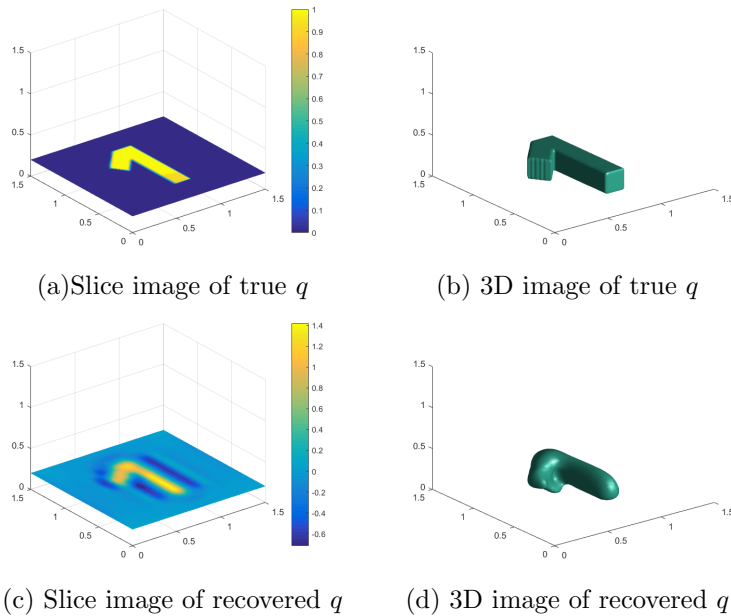


FIG. 8.2. Results of Test 1. Backscattering data, $S = S_{bsc}$. Imaging of '1' shaped q with $q = 1$ in it and $q = 0$ outside. (a) and (b) Correct images. (c) and (d) Computed images.

Test 7. We test the reconstruction by our method of the case when the shape of our inclusion is the same as the shape of the letter 'C'. The function $q(\mathbf{x})$ is depicted on Figures 8.8 (a) and (b). $q = 1$ inside of 'C' and $q = 0$ outside. See Figures 8.8 for the reconstruction results.

Test 8. In this test, we act the same way as in test 4, except that we have replaced the surface $S = S_{bsc}$ with $S = S_{tr}$. The function q is depicted in Figures 8.9 (a) and (b). We took the noise level $\delta = 0.05$, i.e. 5%. Figures 8.9 display the reconstruction results.

REFERENCES

- [1] A.B. BAKUSHINSKII AND A.S. LEONOV, Low-cost numerical method for solving a coefficient inverse problem for the wave equation in three-dimensional space, *Computational Mathematics and Mathematical Physics*, 58, 548-561, 2018.
- [2] A.B. BAKUSHINSKII AND A.S. LEONOV, *Numerical solution of an inverse multifrequency problem in scalar acoustics*, *Computational Mathematics and Mathematical Physics*, 60 (2020), 987-999.
- [3] L. BEILINA AND M.V. KLIBANOV, *Approximate Global Convergence and Adaptivity for Coefficient Inverse Problems*, Springer, New York, 2012.
- [4] L. BOURGEOIS AND J. DARDÉ, *A quasi-reversibility approach to solve the inverse obstacle problem*, *Inverse Problems and Imaging*, 4 (2010), 351-377.
- [5] L. BOURGEOIS AND A. RECOQUILLAY, *A mixed formulation of the Tikhonov regularization and its application to inverse PDE problems*, *ESAIM: Mathematical Modelling and Numerical Analysis*, 52 (2018), 123-145.
- [6] D. COLTON AND R. KRESS, *Inverse Acoustic and Electromagnetic Scattering Theory*, Springer, New York, 1992.
- [7] I.M. GEL'FAND AND B.M. LEVITAN, *On the determination of a differential equation from its spectral function*, *Izvestia Academy Nauk SSSR, Ser. Math.*, 15 (1951), 309-360.
- [8] P. GUILLEMENT AND R.G. NOVIKOV, *Inversion of weighted Radon transforms via finite Fourier series weight approximation*, *Inverse Problems in Science and Engineering*, 22 (2013), 787-

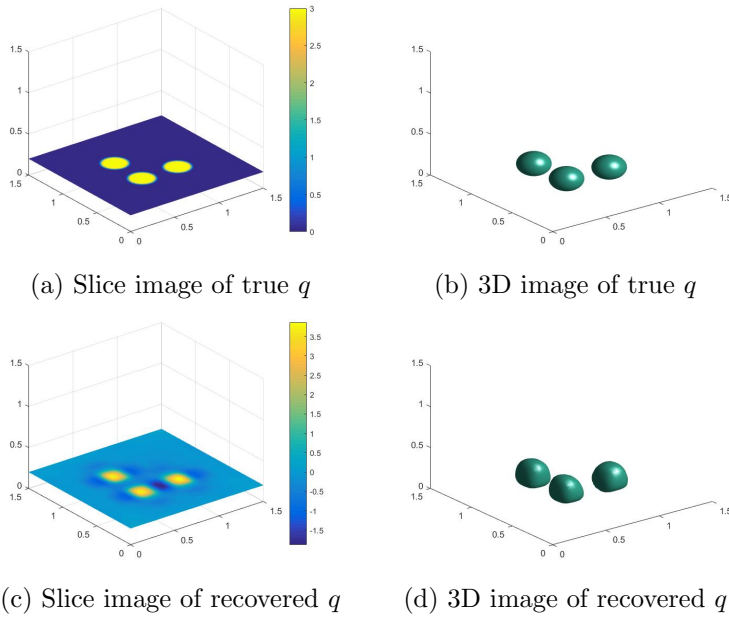


FIG. 8.3. Results of Test 2. Backscattering data, $S = S_{bsc}$. Imaging of three ball shaped inclusions with $q = 3$ in each of them and $q = 0$ outside. a) and b) Correct images. c) and d) Computed images.

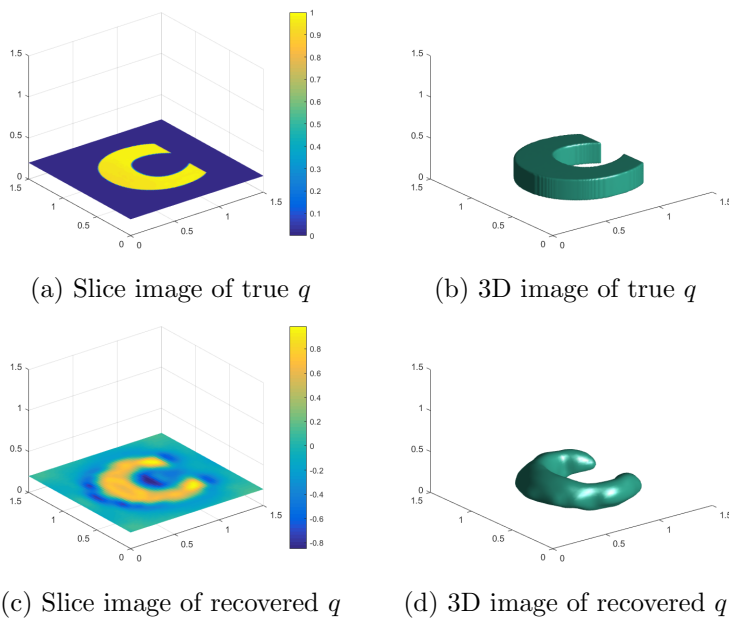


FIG. 8.4. Results of Test 3. Backscattering data, $S = S_{bsc}$. Imaging of 'C' shaped q with $q = 1$ in it and $q = 0$ outside. (a) and (b) Correct images. (c) and (d) Computed images.

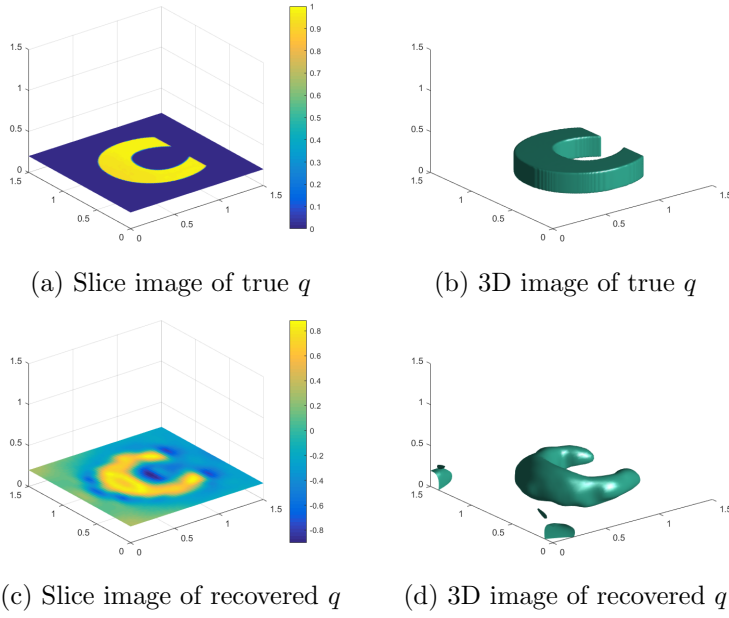


FIG. 8.5. Results of Test 4. Backscattering data, $S = S_{bsc}$. Imaging of 'C' shaped q with $q = 1$ in it and $q = 0$ outside. (a) and (b) Correct images. (c) and (d) Computed images. In this case, noise level $\delta = 0.05$ (i.e.5%).

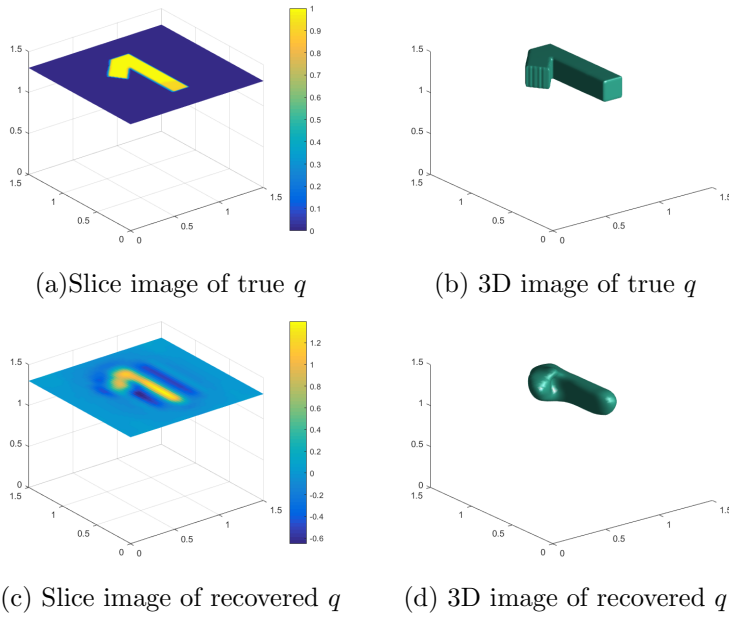


FIG. 8.6. Results of Test 5. Transmitted data, $S = S_{tr}$. Imaging of '1' shaped q with $q = 1$ in it and $q = 0$ outside. (a) and (b) Correct images. (c) and (d) Computed images.

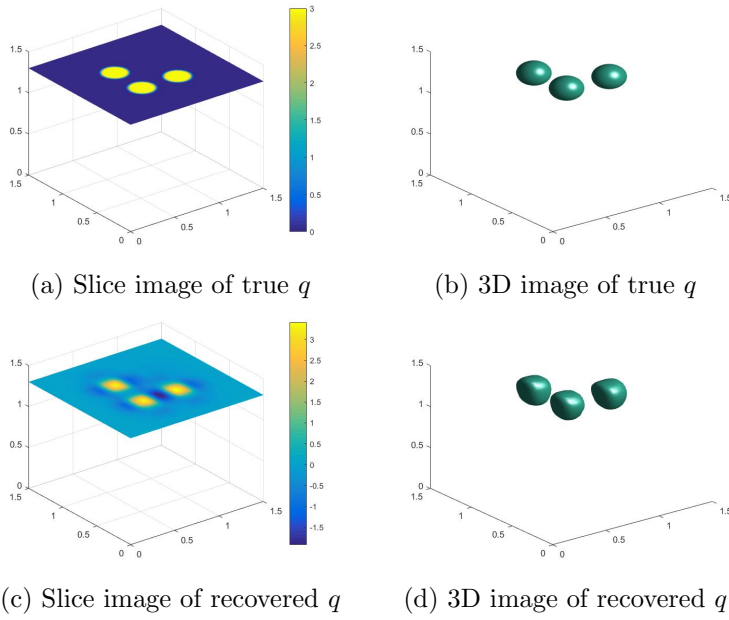


FIG. 8.7. Results of Test 6. Transmitted data, $S = S_{tr}$. Imaging of 3 ball shaped inclusions with $q = 3$ in each of them and $q = 0$ outside. a) and b) Correct images. c) and d) Computed images.

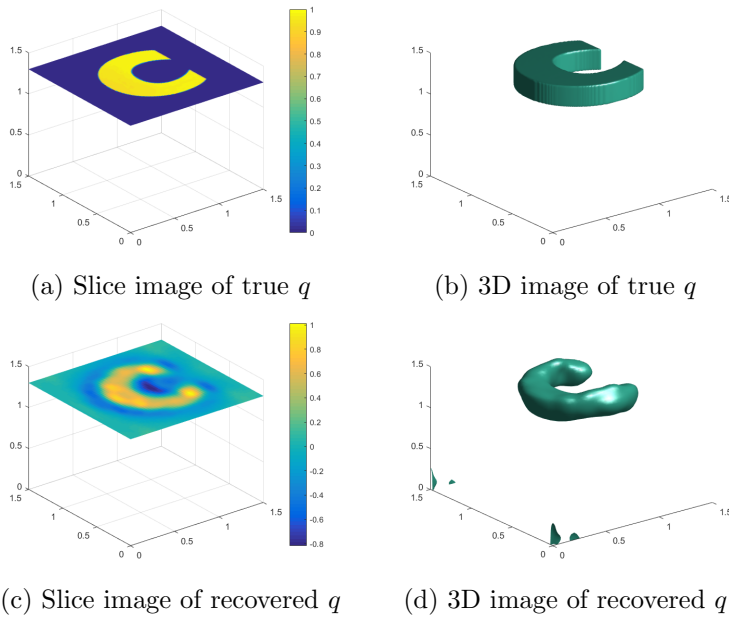


FIG. 8.8. Results of Test 7. Transmitted data, $S = S_{tr}$. Imaging of 'C' shaped q with $q = 1$ in it and $q = 0$ outside. (a) and (b) Correct images. (c) and (d) Computed images.

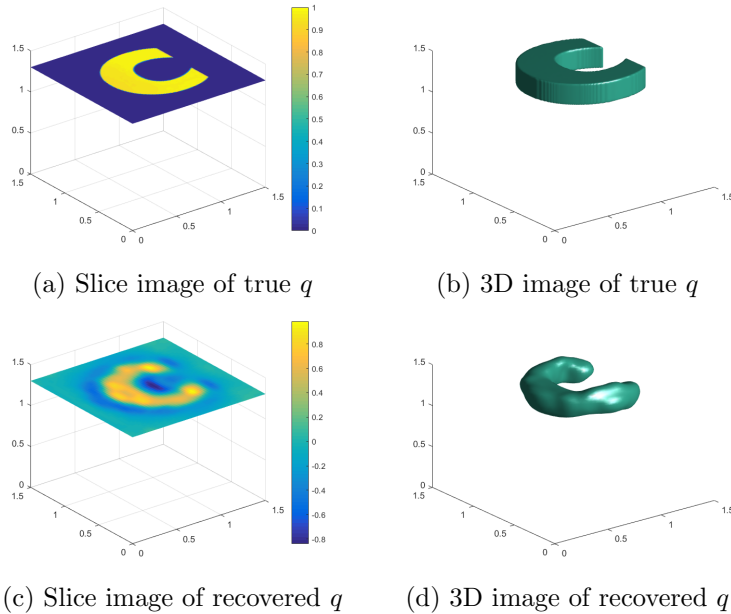


FIG. 8.9. Results of Test 8. Transmitted data, $S = S_{tr}$. Imaging of 'C' shaped q with $q = 1$ in it and $q = 0$ outside. (a) and (b) Correct images. (c) and (d) Computed images. In this case, noise level $\delta = 0.05$ (i.e.5%).

802.

- [9] S.I. KABANIKHIN, A.D. SATYBAEV AND M.A. SHISHLENIN, *Direct Methods of Solving Multidimensional Hyperbolic Inverse Problems*, VSP, Utrecht, 2004.
- [10] S.I. KABANIKHIN, K.K. SABELFELD, N.S. NOVIKOV AND M.A. SHISHLENIN, *Numerical solution of the multidimensional Gelfand–Levitan equation*, *J. Inverse and Ill-Posed Problems*, 23 (2015), 439-450.
- [11] S.I. KABANIKHIN, N.S. NOVIKOV, I. V. OSEDELETS AND M.A. SHISHLENIN, *Fast Toeplitz linear system inversion for solving two-dimensional acoustic inverse problem*, *J. Inverse and Ill-Posed Problems*, 23 (2015), 687-700.
- [12] V. A. KHOA, M. V. KLIBANOV AND L. H. NGUYEN, *Convexification for a three-dimensional inverse scattering problem with the moving point source*, *SIAM Journal on Imaging Sciences*, 13, 871-904, 2020.
- [13] V. A. KHOA, G. W. BIDNEY, M. V. KLIBANOV, LOC H. NGUYEN, LAM H. NGUYEN, A. J. SULLIVAN AND V. N. ASTRATOV, *Convexification and experimental data for a 3D inverse scattering problem with the moving point source*, *Inverse Problems*, 36 (2020), 085007.
- [14] V. A. KHOA, G. W. BIDNEY, M. V. KLIBANOV, LOC H. NGUYEN, LAM H. NGUYEN, A. J. SULLIVAN AND V. N. ASTRATOV, *An inverse problem of a simultaneous reconstruction of the dielectric constant and conductivity from experimental backscattering data*, *Inverse Problems in Science and Engineering*, published online, <https://doi.org/10.1080/17415977.2020.1802447>, 2020.
- [15] M. V. KLIBANOV, *Carleman estimates for global uniqueness, stability and numerical methods for coefficient inverse problems*, *J. Inverse and Ill-Posed Problems*, 21 (2013), pp. 477–560.
- [16] M.V. KLIBANOV, *Carleman estimates for the regularization of ill-posed Cauchy problems*, *Applied Numerical Mathematics*, 94 (2015), 46-74.
- [17] M.V. KLIBANOV AND V.G. ROMANOV, *Reconstruction procedures for two inverse scattering problems without the phase information*, *SIAM J. Appl. Math.*, 76, 178-196, 2016.
- [18] M.V. KLIBANOV, *Convexification of restricted Dirichlet-to-Neumann map*, *J. Inverse and Ill-Posed Problems*, 25 (2017), pp. 669-685.
- [19] M. V. KLIBANOV, J. LI AND W. ZHANG, *Electrical impedance tomography with restricted Dirichlet-to-Neumann map data*, *Inverse Problems*, 35 (2019), 035005.
- [20] M. V. KLIBANOV, J. LI AND W. ZHANG, *Convexification for the inversion of a time dependent*

- wave front in a heterogeneous medium*, SIAM J. Appl. Math., 79 (2019), 1722-1747.
- [21] M. V. KLIBANOV, A. E. KOLESOV AND D.-L. NGUYEN, *Converification method for an inverse scattering problem and its performance for experimental backscatter data for buried targets*, SIAM J. Imaging Sciences, 12 (2019), 576–603.
 - [22] M.V. KLIBANOV AND L.H. NGUYEN, *PDE-based numerical method for a limited angle X-ray tomography*, Inverse Problems, 35 (2019), 045009.
 - [23] M. V. KLIBANOV, *Travel time tomography with formally determined incomplete data in 3D*, *Inverse Problems and Imaging*, 13, 1367-1393, 2019.
 - [24] M. V. KLIBANOV, *On the travel time tomography problem in 3D*, *J. Inverse and Ill-Posed Problems*, 27, 591-607, 2019.
 - [25] M.V. KLIBANOV, T.T. LE AND L.H. NGUYEN, *Convergent numerical method for a linearized travel time tomography problem with incomplete data*, *SIAM J. Scientific Computing*, 42 (2020), B1173-B1192.
 - [26] M.V. KLIBANOV, A.V. SMIRNOV, K.A. VO, A.J. SULLIVAN AND L.H. NGUYEN, *Through-the-Wall nonlinear SAR imaging*, arXiv: 2008.12662v3, 2020.
 - [27] R. LATTES, J.-L. LIONS, *The Method of Quasireversibility: Applications to Partial Differential Equations*, Elsevier, New York, 1969.
 - [28] M.M. LAVRENT'EV, *On an inverse problem for the wave equation*, Soviet Mathematics Doklady, 5 (1964), 970-972.
 - [29] M.M. LAVRENT'EV, V. G. ROMANOV AND S.P. SHISHATSKII, *Ill-Posed Problems of Mathematical Physics and Analysis*, AMS, RI, 1986.
 - [30] B.M. LEVITAN, *Inverse Sturm-Liouville Problems*, VNU Science, Utrecht, The Netherlands, 1987.
 - [31] L. NGUYEN, M. RESSLER AND J. SICHINA, *Sensing through the wall imaging using the Army Research Lab ultra-wideband synchronous impulse reconstruction (UWB SIRE) radar*, Proc. SPIE, Vol. 6047, 6947/0B, 2008
 - [32] A. G. RAMM, *Inverse scattering for geophysical problems*, *Physics Letters*, 99A, 258-260, 1983.
 - [33] V. G. ROMANOV, *Inverse Problems of Mathematical Physics*. VNU Press, Utrecht, 1986.
 - [34] A. V. SMIRNOV, M. V. KLIBANOV, AND L. H. NGUYEN, *On an inverse source problem for the full radiative transfer equation with incomplete data*, *SIAM Journal on Scientific Computing*, 41, B929–B952, 2019.
 - [35] A.N. TIKHONOV, A.V. GONCHARSKY, V.V. STEPANOV AND A.G. YAGOLA, *Numerical Methods for the Solution of Ill-Posed Problems*, Kluwer, London, 1995.
 - [36] B.R. VAINBERG, *Principles of radiation, limiting absorption and limiting amplitude in the general theory of partial differential equations*, *Russian Math. Surveys*, 21 (1966), pp. 115–193.
 - [37] B.R. VAINBERG, *Asymptotic Methods in Equations of Mathematical Physics*, Gordon and Breach, New York, 1989.